



HAL
open science

Fossil evidence for serpentinization fluids fueling chemosynthetic assemblages

Franck Lartaud, Crispin T.S. Little, Marc de Rafelis, Germain Bayon, Jerome Dymont, Benoit Ildefonse, Vincent Gressier, Yves Fouquet, Françoise Gaill,
Nadine Le Bris

► **To cite this version:**

Franck Lartaud, Crispin T.S. Little, Marc de Rafelis, Germain Bayon, Jerome Dymont, et al.. Fossil evidence for serpentinization fluids fueling chemosynthetic assemblages. Proceedings of the National Academy of Sciences of the United States of America, 2011, 108, pp.7698-7703. 10.1073/pnas.1009383108 . insu-01352929

HAL Id: insu-01352929

<https://insu.hal.science/insu-01352929v1>

Submitted on 10 Aug 2016

HAL is a multi-disciplinary open access archive for the deposit and dissemination of scientific research documents, whether they are published or not. The documents may come from teaching and research institutions in France or abroad, or from public or private research centers.

L'archive ouverte pluridisciplinaire **HAL**, est destinée au dépôt et à la diffusion de documents scientifiques de niveau recherche, publiés ou non, émanant des établissements d'enseignement et de recherche français ou étrangers, des laboratoires publics ou privés.

Fossil evidence for serpentinization fluids fueling chemosynthetic assemblages

Franck Lartaud^{a,b,1}, Crispin T. S. Little^c, Marc de Rafelis^b, Germain Bayon^d, Jerome Dymont^e, Benoit Ildefonse^f, Vincent Gressier^b, Yves Fouquet^d, Françoise Gaill^g, and Nadine Le Bris^{a,h}

^aUniversité Pierre et Marie Curie–Paris 6, Laboratoire d'Ecogéochimie des Environnements Benthiques, Centre National de la Recherche Scientifique, Laboratoire Arago, 66650 Banyuls-sur-Mer, France; ^bUniversité Pierre et Marie Curie–Paris 6, Institut des Sciences de la Terre de Paris, Laboratoire Biominéralisations et Environnements Sédimentaires, Centre National de la Recherche Scientifique 75252 Paris Cedex 05, France; ^cSchool of Earth and Environment, University of Leeds, Leeds LS2 9JT, United Kingdom; ^dDépartement Géosciences Marines, Institut Français de Recherche pour l'Exploitation de la Mer, Centre de Brest, 29280 Plouzané, France; ^eInstitut de Physique du Globe de Paris, Centre National de la Recherche Scientifique, Equipe Géosciences Marines, 75252 Paris Cedex 05, France; ^fGéosciences Montpellier, Centre National de la Recherche Scientifique, Université Montpellier 2, 34095 Montpellier Cedex 05, France; ^gCentre National de la Recherche Scientifique, Institut Écologie et Environnement, Université Pierre et Marie Curie, Institut de Recherche pour le Développement, Muséum National d'Histoire Naturelle, 75252 Paris Cedex 05, France; and ^hLaboratoire Environnements Profonds, Institut Français de Recherche pour l'Exploitation de la Mer, Centre de Brest, 29280 Plouzané, France

Edited by Norman H. Sleep, Stanford University, Stanford, CA, and approved March 24, 2011 (received for review June 30, 2010)

Among the deep-sea hydrothermal vent sites discovered in the past 30 years, Lost City on the Mid-Atlantic Ridge (MAR) is remarkable both for its alkaline fluids derived from mantle rock serpentinization and the spectacular seafloor carbonate chimneys precipitated from these fluids. Despite high concentrations of reduced chemicals in the fluids, this unique example of a serpentine-hosted hydrothermal system currently lacks chemosynthetic assemblages dominated by large animals typical of high-temperature vent sites. Here we report abundant specimens of chemosymbiotic mussels, associated with gastropods and chemosymbiotic clams, in approximately 100 kyr old Lost City-like carbonates from the MAR close to the Rainbow site (36°N). Our finding shows that serpentinization-related fluids, unaffected by high-temperature hydrothermal circulation, can occur on-axis and are able to sustain high-biomass communities. The widespread occurrence of seafloor ultramafic rocks linked to likely long-range dispersion of vent species therefore offers considerably more ecospace for chemosynthetic fauna in the oceans than previously supposed.

Bathymodiolus | Ghost City | ultramafic-hosted | mid-ocean ridge | ecogeochemistry

High-temperature hydrothermal vents occur at very geographically restricted sites in the deep-sea, localized on spreading ridges and arc-related volcanoes. Typically, such vent fluids are metal- and H₂S-rich and precipitate metallic sulfide chimneys on the seafloor (1, 2). These vents usually support high-biomass invertebrate communities, dominated by a small number of endemic species forming symbioses with diverse chemoautotrophic bacteria (e.g., siboglinid tubeworms, bresiliid shrimp, provaniid gastropods, vesicomysid clams, and bathymodiolin mussels) (1, 3). These symbioses exploit chemical energy from a variety of fluids enriched in reduced compounds, mostly hydrogen sulfide and methane, to fix carbon (4). Along slow and ultraslow spreading ridges, like the Mid-Atlantic Ridge (MAR), ultramafic mantle rocks can be exposed on the seafloor by large offset faults (5). Seawater serpentinization of these peridotites produces hydrogen, which subsequently reacts with CO₂ to form methane (6, 7). Because of this, peridotite-hosted high-temperature vent sites on the MAR (e.g., Rainbow and Logatchev) exhibit elevated levels of methane and hydrogen contents in their fluids. Hydrothermal activity can also occur at off-axis ridge settings. A unique example of this is the Lost City vent field, discovered in the year 2000 on the Atlantis Massif, 30°07'N MAR, at 750- to 850-m depth (8). Here, exothermic serpentinization processes may largely drive the hydrothermal convection, although a contribution of magmatic inputs is not excluded (9). The main difference between this off-axis vent field and the other known vent fields on the MAR-axis is that the majority of the Lost City

vent fluids are metal-poor, low-temperature (40–91 °C), and have high pH (9–11). Further, the Lost City fluids are also highly enriched in H₂ and CH₄ and comparatively lower in H₂S (10). On contact with ambient seawater these alkaline fluids precipitate chimney structures up to 60 m high composed of carbonates (aragonite and calcite) and brucite (Mg(OH)₂) (11–13). Sulfide minerals are mostly absent from these chimneys, contrasting strongly with on-axis hydrothermal vent structures (13, 14). The Lost City site has generated considerable interest because this sort of system was likely to have been common in early Earth history and represents a plausible geochemical environment for the emergence of life on this, and potentially other, planets (15, 16).

In the context of the MAR peridotite-hosted vent fields another remarkable feature of Lost City is the lack of typical high-biomass animal assemblages dominated by large chemosynthetic invertebrates: There are currently no *Bathymodiolus* mussel beds or bresiliid shrimp swarms, although the diversity of other invertebrates (particularly small gastropods and polychaete worms) is described as being equivalent to that of high-temperature MAR vent communities (11, 17). Only two living specimens of *Bathymodiolus* aff. *azoricus* have been found at Lost City (18, 19), whereas hundreds of broken shell fragments downslope away from the active chimney areas (19, 20) suggest that the population size might have been much larger in the past and is now almost extinct (19). Dead *B. azoricus* shells have also been recently reported from carbonate chimneys at an inactive site near Lost City (21).

Supporting these observations, the enrichment of reduced compounds in Lost City hydrothermal fluid indicates that these, and similar peridotite-hosted vents, hold the energetic potential to support large aggregations of *Bathymodiolus* mussels, a genus widely distributed along the MAR axis (22). *B. aff. azoricus* at Lost City hosts the same symbiont phylotypes as the methanotrophic and thiotrophic endosymbionts of both *B. azoricus* and *B. puteoserpentis* from on-axis sites on the MAR (18), where the methanotrophic symbiont fixes carbon from methane and the chemolithoautotroph uses sulfide to fix CO₂ (23–25). In addition to methane, DeChaine et al. (18) suggest that *B. aff. azoricus* at Lost City could also be utilizing hydrogen, although hydrogen-oxidizing symbionts have yet to be identified. These authors further

Author contributions: F.L., M.d.R., J.D., B.I., Y.F., F.G., and N.L.B. designed research; F.L., C.T.L., M.d.R., G.B., and V.G. performed research; F.L., C.T.L., M.d.R., G.B., and N.L.B. analyzed data; and F.L., C.T.L., and N.L.B. wrote the paper.

The authors declare no conflict of interest.

This article is a PNAS Direct Submission.

¹To whom correspondence should be addressed. E-mail: franck.lartaud@obs-banyuls.fr.

This article contains supporting information online at www.pnas.org/lookup/suppl/doi:10.1073/pnas.1009383108/-DCSupplemental.

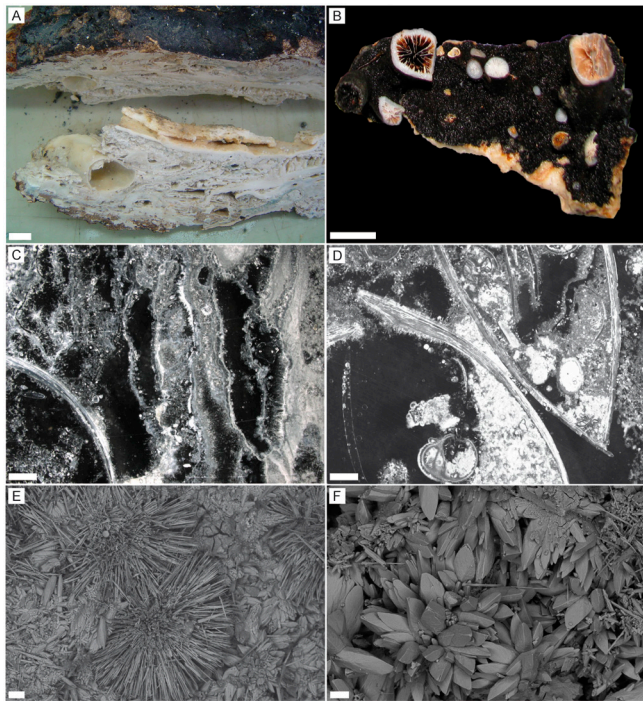


Fig. 2. Carbonate samples from Ghost City. (A) Sectioned block formed of authigenic carbonate cements covered by ferric oxyhydroxide dark crust upon which (B) solitary corals have grown. (Scale bars, 1 cm.) (C) Photomicrograph showing anastomosing aragonite laminae defining fluid flow channels (center and right) and a piece of mussel shell (bottom left). The channels have thin aragonite walls, some with thin collomorphic coatings; others are in-filled with micritic carbonate. A thin rim of aragonite acicular crystals seems to be the latest cement phase, covering mussel shells, channel walls (top left), and micritic infill (center right). (Scale bars, 1 mm.) (D) Photomicrograph showing articulated mussel specimens and gastropods enclosed within authigenic carbonate. (Scale bars, 1 mm.) (E and F) SEM photomicrographs of carbonates showing aragonite acicular crystals (E) and rosette of glendonite crystals (F). (Scale bars, 20 μ m.)

Ghost City carbonate formation is significantly older than the first evidence of Rainbow vent activity (23 ± 1.5 kyr) (33). Additionally, the same carbonate sample exhibits a radiogenic strontium isotopic ratio ($^{87}\text{Sr}/^{86}\text{Sr}$) of 0.70916 ± 0.00006 , close to seawater ratios.

Among known authigenic carbonates from oceanic environments where ultramafic rocks are exposed, such as vein-filling aragonites in serpentinites (34, 35), samples from Ghost City are texturally and mineralogically most similar to those from Lost City, particularly the carbonates of old (up to 25 kyr) inactive chimneys (12). According to these authors, the Lost City inactive structures display well-defined fluid flow paths, retaining significant porosity (up to approximately 35%) and are characterized by dark or black exteriors that contrast to white, ivory, or gray interiors. The outer walls of these structures become dark due to

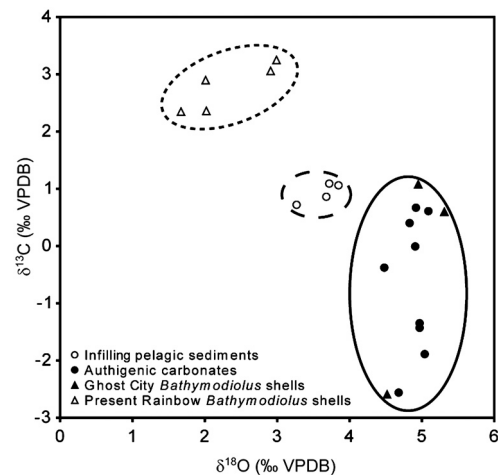


Fig. 3. Oxygen and carbon isotopic composition of Ghost City carbonates and *Bathymodiolus* shells and living *Bathymodiolus* shells from the Rainbow hydrothermal vent field. Domains limited by lines represent the scatterplot of canonical scores obtained by applying discriminant functions to the data.

manganese precipitation associated with aging and are colonized by serpulid worms and corals (13). In older inactive chimneys the internal microchannels are progressively in-filled with micritic calcite; brucite, which is undersaturated in seawater, tends to disappear in these chimneys (12). Another feature indicative of prolonged postformation interaction with seawater is near seawater Sr isotope values in carbonate minerals, as seen in both the Lost City inactive chimneys (13) and Ghost City samples. One mineralogical distinction of Ghost City carbonates is the presence of glendonite. Glendonite in Ghost City carbonate crust exhibits a characteristic star shape and is associated with acicular aragonite crystals surrounding the benthic fossils. Glendonite is a pseudomorph after ikaite, a very unstable hydrous calcium carbonate associated with cold water ($<6^\circ\text{C}$) depositional systems, including glaciomarine and deep water settings (36, 37). Original ikaite precipitation is favored by elevated alkalinity, high pH (>10) and dissolved phosphate enrichments. Glendonite was not reported in Lost City carbonates, but the presence of ikaite in the walls of active chimneys was suspected from the observation of rapid dissolution of elongated carbonate crystals during sampling (13).

The oxygen and carbon isotope values of the Ghost City authigenic carbonates are consistent with those observed in serpentinization contexts. The ^{18}O enrichment during fluid/rock interaction results in carbonates with high $\delta^{18}\text{O}$ values ($>2\text{‰}$) (11, 38). The Ghost City carbon isotope signatures ($\delta^{13}\text{C} = -2.6$ to 0.7‰) are comparable to those measured in carbonates from serpentinite-hosted systems, like the South Chamorro Seamount ($\delta^{13}\text{C} = -2.1$ to -1.3‰) and the Conical Seamount ($\delta^{13}\text{C} = -2.9$ to -0.1‰) in the Mariana forearc (39–41), and lie within the wide range of carbonate isotopic signatures reported for Lost City (-7 to $+13\text{‰}$) (11). Carbonates with the lower

Table 1. Mean, standard deviation, and range of oxygen and carbon isotopic compositions of carbonates and mussel shells

	(n)	$\delta^{18}\text{O} \pm \text{SD}$ (‰ VPDB)	Min/Max	$\delta^{13}\text{C} \pm \text{SD}$ (‰ VPDB)	Min/Max
GHOST CITY					
In-filled pelagic sediments	4	3.63 ± 0.25	3.27/3.85	0.93 ± 0.17	0.72/1.09
Authigenic carbonates	9	4.88 ± 0.19	4.48/5.09	-0.66 ± 1.18	-2.56/0.67
<i>Bathymodiolus</i> shells	3	4.93 ± 0.40	4.52/5.31	-0.30 ± 1.99	-2.59/1.08
LOST CITY					
Vent carbonates (11)	50		-6/5		-7/13
Methane (11, 44, 45)				-11.9	-13.6/-8.8
RAINBOW					
Living <i>Bathymodiolus</i> shells	5	2.32 ± 0.59	1.67/2.99	2.78 ± 0.41	2.35/3.25
Methane (44)					-17.7/-15.8

Comparison of carbonates and mussel shells from Ghost City, Lost City, and Rainbow high-temperature hydrothermal vent site.

Table 2. U-Th ages for Ghost City carbonate samples

Sample	Corrected U-Th age (kyr) ± 2σ	Initial δ ²³⁴ U (‰) ± 2σ
S1	195 ± 11	183 ± 10
S2	110 ± 0.9	150 ± 1
S3	65 ± 11	170 ± 1
S4	46 ± 0.3	129 ± 1

isotopic signature reflect a mixed inorganic carbon source with contributions from seawater ($\delta^{13}\text{C}_{\text{DIC}} \sim 0\text{‰}$) and an isotopically lighter-DIC source. Owing to the very low concentration of inorganic carbon in serpentinization fluids, the most likely origin for this ^{13}C depleted DIC is the oxidation of methane. Methane in serpentinization fluids are characterized by light carbon isotopic signatures (e.g., $\delta^{13}\text{C}_{\text{CH}_4} = -7\text{‰}$ in the Zambales ophiolite, -10.3‰ at Logatchev, -16.7‰ at Rainbow, and -11.9‰ at Lost City) (42–45), which can be further fractionated by methanotrophic microbes converting methane into inorganic carbon. While abiotic methane oxidation is kinetically inhibited at low temperature (46), microbial oxidation of methane can occur in subsurface habitats with various electron acceptors (e.g., oxygen and sulfate) during the mixing of seawater with end-member fluids (47, 48). According to Proskurowski et al. (48), the fractionation factor resulting of anaerobic or aerobic methane oxidation can be as high as 1.039 (49, 50) and will result in further depletion of the initial carbon isotopic ratio by at least -13‰ . Only a small fraction (approximately 5%) of this ^{13}C depleted methane is thus sufficient to explain the slightly negative carbon isotopic signature of some Ghost City carbonates. An additional contribution from biogenic methane formed during the subsurface mixing of seawater and the end-member fluid, as described in Proskurowski et al. (48), cannot be ruled out. This assumption is supported by the identification of both methanogenic and anaerobic methane-oxidizing Archaea at Lost City, particularly in the less active chimneys where seawater mixing is occurring (28). In Lost City-type conditions, seawater is the only source of HCO_3^- , and mixing is required to compensate the poor supply of this ion from the fluid. As a consequence, the substantial isotopic fractionation resulting of biogenic methane formation that was observed at basalt-hosted diffuse vents (48) may not be achieved due to limiting inorganic carbon conditions. The relative importance of biogenic methane is therefore difficult to estimate from Ghost City samples' isotopic ratios.

The geological context, as well as petrographic and isotopic data, provides supporting evidence that the Ghost City carbonates were formed 110,000 years ago from venting of metal-poor fluids. Despite the proximity with the Rainbow high-temperature vents field, the lack of polymetallic sulfide precipitates in the Ghost City carbonate samples precludes a high-temperature metal-rich hydrothermal fluid contribution in their formation. More likely, these fluids were formed from low-temperature hydrothermal circulation related to serpentinization and were probably close in composition to those currently venting at Lost City.

Ghost City Fossils

We counted 146 specimens of the mussel *Bathymodiolus* aff. *azoricus* on the exposed surfaces of the eight Ghost City carbonate blocks (Fig. 4 and Fig. S4). The shells range in length from 5 mm to 84 mm, which is comparable to living *B. azoricus* shells from high-temperature hydrothermal vent fields on the MAR (51). Very few of the Ghost City mussel shells are fragmented, and quite a few specimens have articulated valves, with a ratio of 3.6 disarticulated to articulated shells ($n = 73$). Some of the small articulated mussel shells are nested within larger articulated specimens (Fig. 2D). These features are indicative of in situ growth and a lack of post mortem transport. This interpretation is supported by the isotope composition of the Ghost City *B. aff.*

azoricus shells ($\delta^{18}\text{O} = 4.93 \pm 0.40\text{‰}$, $\delta^{13}\text{C} = -0.30 \pm 1.99\text{‰}$, $n = 3$; Table 1), values that are more similar to the Ghost City authigenic carbonates than living *Bathymodiolus* shells from the Rainbow high-temperature hydrothermal vent site (CDA analysis; Fig. 3 and Table S2). The other benthic fossils enclosed within the Ghost City carbonate samples (Fig. 4) comprise serpulid tubes (>30); the vesicomyid clam *Phreagena* sp. ($n = 2$); the thyasirid clam *Thyasira* sp. ($n = 1$); the limpet *Paralepetopsis* aff. *ferrugivora* ($n = 15$); and the snails *Protolira* aff. *thorvaldssoni* ($n = 32$), *Phymorhynchus* sp. ($n = 1$), *Anatoma* sp. ($n = 2$), and *Lurifax vitreus* ($n = 1$). These also show variable preservation, but in general the shells that were originally aragonitic (the gastropods and clams) show more dissolution and recrystallization than the mixed calcite/aragonite mussel shells, an observation consistent with prolonged seawater interaction (Fig. S5). The Ghost City mollusk assemblage shares five taxa with living MAR axial high-temperature vent communities (3, 52–54), including two locally at Rainbow (*Bathymodiolus* and *Protolira*), and two taxa associated with sedimented vent sites (Table S3). The Ghost City *Phreagena* sp. is also found at the recently described Clamstone site, an inactive (approximately 25 kyr BP) serpentine-hosted sedimented vent field near Rainbow (approximately 1.2 km east of Ghost City, at a depth of 1,980 m) (55). Thyasirid clams that may be conspecific with the Ghost City *Thyasira* sp. occur at Clamstone (55), Anya's Garden, a sedimented vent site in the Logatchev area (52, 56, 57), and have also been reported in

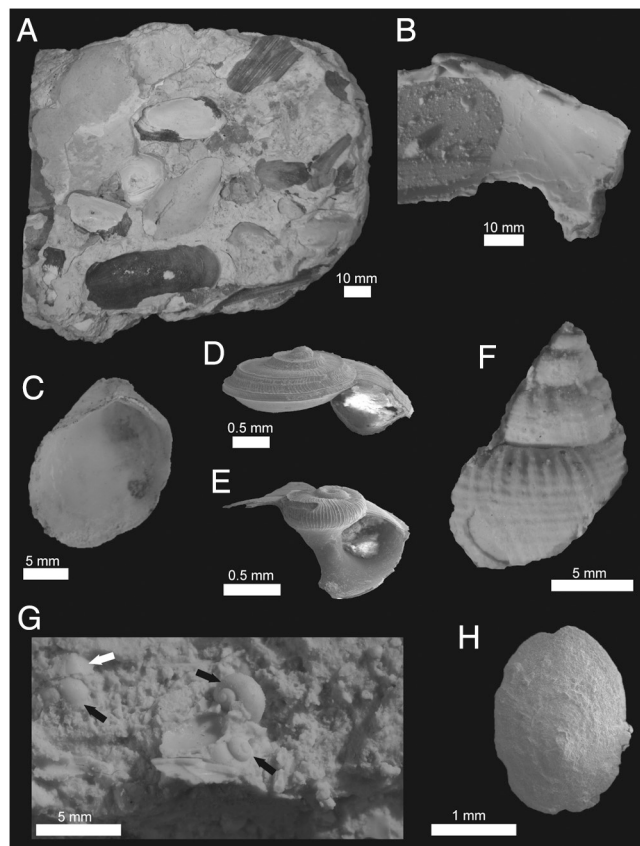


Fig. 4. Fossils from Ghost City carbonates. (A) Carbonate block with numerous specimens of *Bathymodiolus* aff. *azoricus*, showing varying degrees of shell preservation. (B) Silicone rubber cast of vesicomyid bivalve *Phreagena*, right valve interior. (C) Thyasirid bivalve, left valve interior. (D) Gastropod *Lurifax vitreus*, oblique apertural view. (E) Gastropod *Anatoma* sp., oblique view of damaged specimen. (F) Silicone rubber cast of gastropod *Phymorhynchus* sp., side view. (G) Silicone rubber cast from carbonate containing three *Protolira* aff. *thorvaldssoni* gastropod specimens (black arrows) and a single limpet (white arrow). (H) Limpet *Paralepetopsis* aff. *ferrugivora*, abapertural view of slightly corroded specimen.

soft sediments at Lost City (20). Thus, the Ghost City mollusk fauna is a mixture of MAR vent species from sedimented sites and more typical chimney habitat mussel bed communities. Although Ghost City fauna has a higher biomass, the mollusk species list is not greatly different from Lost City communities, with three mollusk species shared between the two sites: *B. azoricus*, *Thyasira* species, and the gastropod *Lurifax* (see Table S3).

High-Biomass Vent Communities Supported by Serpentinization Fluids

The Ghost City carbonates demonstrate that (i) high-biomass populations of *Bathymodiolus* mussels and other symbiont-hosting mollusks can be supported by metal-depleted and likely alkaline fluids, similar to the serpentinization-related vent fluids described at Lost City; and (ii) these communities have been present on the axis of the MAR for at least 110,000 years. The flexible *B. azoricus* dual symbiosis responds to variations in the methane-to-sulfide ratio in the environment (24, 25), making this species particularly well adapted to the variety of fluid chemistries that are found on the MAR (8, 58). The Ghost City fossil mussels might therefore also have relied on methanotrophy and, potentially, on sulfide, or even hydrogen, oxidation as primary energy pathways. Although the geological setting is different, there is evidence that some other *Bathymodiolus* species are able to exploit diverse energy sources present in a serpentinization context. At the South Chamorro serpentinite seamount in the Mariana forearc, mussels thrive in sedimented cracks in seafloor carbonate cement, and based on soft tissue carbon and sulfur isotopic data, Yamanaka et al. (41) suggest that the mussels host both methanotrophic and thiotrophic symbionts, utilizing both methane from serpentinization reactions and sulfur produced by sulfate reducing bacteria in the sediment. Additionally, vesicomids (4, 59) and many of the studied large thyasirid (4, 52) species host sulfide-oxidizing symbionts, and the presence of representative species in the Ghost City carbonates suggests that a threshold amount of sulfide was present in the Ghost City environment.

Implications

It is unclear why communities of symbiont-hosting mollusks, including high densities of large *Bathymodiolus* mussels, do not currently persist at Lost City, when they have been present in the past as shown by accumulations of dead shells. Because *Bathymodiolus azoricus* is able to exploit variable chemical energy sources, the most likely explanation is to be searched for in the ecological processes that govern community dynamics in fragmented habitats. One possible cause of this extinction may be related to the dispersal potential of vent species. Lost City is located further from the ridge axis than Ghost City and may have lacked of sufficient larval flow from high-temperature Rainbow-like vent field communities after a major disturbance event. Another explanation could be that the focused flow chimney complex at Lost City lacks the mild temperature diffuse flow areas (<15 °C) with substantial concentrations of electron donors like methane or sulfide, that characterize suitable habitat for vent mussels (22). Further investigation of Lost City habitat conditions and population genetics will help discriminating between these hypotheses.

The findings further support the hypothesis of a widespread occurrence of hydrothermal fluid circulation hosted in exposed ultramafic rocks on the ocean floor (60). The estimated duration of serpentinization-related fluid venting (over 10 kyr to 100 kyr time scales) (32) contrasts strongly with the geographically restricted and short-lived high-temperature vent fields known

to date. Our results indicate that exposed mantle rocks undergoing serpentinization could host deep-sea chemosynthetic vent communities in a wide range of geological settings, including slow and ultraslow spreading ridge axes, off-axis Oceanic Core Complexes (61), continental margins (62), and serpentinite seamounts in forearc settings (63). The exploration of ultramafic rock exposures in the deep sea is thus a fertile area for the understanding both long-range larval dispersal of vent species and the specific requirements for settlement and growth of chemosynthetic animals.

Methods

XRD Analyses. Analyses of carbonate matrix, oxide crust, and mussel shells were made at the ITeP laboratory (UPMC Univ Paris 06) on a Siemens D501. *Bathymodiolus* aff. *azoricus* mussel shells were scrubbed in distilled water with a toothbrush immediately upon collection to remove loosely attached biogenic and inorganic particles. Sample powders of original calcitic outer layer and aragonitic inner layer of the shells were drilled from a depth of approximately 0.1 mm.

Optical Petrography. Polished thin sections of carbonates were observed using a stereomicroscope Zeiss SteREO Discovery V20 (Fig. 2 and Fig. S1) Porosity measurements were made using JMicrovision software (www.jmicrovision.com).

Carbon and Oxygen Stable Isotopes Analyses. Analyses of three *Bathymodiolus* aff. *azoricus* shells and 13 carbonate matrix (authigenic carbonate and infilling pelagic sediments) Ghost City samples were made on a VG Micromass 602 mass spectrometer. Additionally, five shells of living *B. azoricus* from the Rainbow vent field were analyzed. Powdered samples from mussel shells for the isotopic analyses (3–4 mg) were obtained from the cleaned outer layer using a rotary drill with a diamond-tipped burr. The shell sample powders were pretreated with 1.5 % NaClO for 30 min to remove organic contaminants, rinsed three times with distilled water following a protocol modified after (64, 65). All carbonate powders were acidified in 100% phosphoric acid at 50 °C under vacuum. The produced CO₂ was collected and analyzed using the mass spectrometer. Isotopic data are reported in conventional delta (δ) notation relative to the Vienna Pee Dee Belemnite (VPDB). The standard used for the analyses was an internal standard calibrated on the NBS-19. Standard deviation for δ¹⁸O and δ¹³C is ±0.10‰.

Uranium/Thorium and Strontium Analyses. Analyses were made in the Pôle Spectrométrie Océan (Brest) on a Neptune MC-ICPMS. For uranium and thorium isotope measurements, about 2 mg of carbonate sample was dissolved in 7.5M HNO₃ and spiked with a mixed ²³⁶U/²²⁹Th spike (66). U and Th were separated chemically using conventional anion exchange techniques adapted from previous studies (67). U and Th concentrations and isotope ratios were then measured in the MC-ICPMS. The carbonate age was corrected for detrital contamination (inherited ²³⁰Th) using measured ²³²Th concentrations and assuming a typical ²³²Th/²³⁰Th ratio (150,000) for the contaminant detrital phase, but this correction was insignificant on the calculated age (about 1%) (68). Strontium was isolated using Sr resin and the isotope ratios were measured using the MC-ICPMS. Isotope ratios were normalized to ⁸⁶Sr/⁸⁸Sr = 0.1194 and corrected from ⁸⁷Rb and ⁸⁶Kr interferences on the ⁸⁷Sr and ⁸⁶Sr signal, respectively.

ACKNOWLEDGMENTS. We thank captain and crew of R/V L'Atalante; the remotely operated vehicle Victor operation group; the MoMARDREAM scientific party for their support during the MoMARDREAM cruise; E. Rongemaille, N.-C. Chu, and E. Ponzevera for analytical work; E. Krylova for vesicomid and thyasirid bivalve identification; and A. Wären for benthic gastropod identification. T.M. Shank and A.L. Meistertzheim are also thanked for their helpful comments. The manuscript also benefited from helpful comments from G. Proskurowski and one anonymous reviewer. Centre National de la Recherche Scientifique (CNRS)-INSU, CNRS-INEE, IFREMER, and GENAVIR are gratefully acknowledged for their financial and technical support. The study was part of the CHEMECO collaborative project from the ESF EUROCORES EURODEEP and benefited from the joint support of Fondation TOTAL and UPMC to the chair "Extreme environment, biodiversity and global change."

1. Van Dover CL (2000) *The Ecology of Deep-Sea Hydrothermal Vents* (Princeton Univ Press, Princeton).
2. Von Damm KL (1990) Seafloor hydrothermal activity: Black smoker chemistry and chimneys. *Annu Rev Earth Planet Sci* 18:173–204.

3. Desbruyères D, Segonzac M, Bright M (2006) *Handbook of Deep-Sea Hydrothermal Vent Fauna—Mollusca* (Denisia, Linz, Austria), pp 141–172.
4. Dubilier N, Bergin C, Lott C (2008) Symbiotic diversity in marine animals: The art of harnessing chemosynthesis. *Nat Rev Microbiol* 6:725–740.

5. Cannat M (1993) Emplacement of mantle rocks in the seafloor at mid-ocean ridges. *J Geophys Res* 98:4163–4172.
6. Abrajano TA, et al. (1988) Methane-hydrogen gas seeps, Zambales Ophiolite, Philippines: Deep or shallow origin? *Chem Geol* 71:211–222.
7. Berndt ME, Allen DE, Seyfried WE, Jr (1996) Reduction of CO₂ during serpentinization of olivine at 300 °C and 500 bar. *Geology* 24:351–354.
8. Kelley DS, et al. (2001) An off-axis hydrothermal vent field near the Mid-Atlantic Ridge at 30°N. *Nature* 412:145–149.
9. Allen DE, Seyfried WE, Jr (2004) Serpentinization and heat generation: Constraints from Lost City and Rainbow hydrothermal systems. *Geochim Cosmochim Acta* 68:1347–1354.
10. Proskurowski G, Lilley MD, Kelley DS, Olson EJ (2006) Low temperature volatile production at the Lost City Hydrothermal Field, evidence from a hydrogen stable isotope geothermometer. *Chem Geol* 229:331–343.
11. Kelley DS, et al. (2005) A serpentinite-hosted ecosystem: The Lost City hydrothermal field. *Science* 307:1428–1434.
12. Früh-Green GL, et al. (2003) 30,000 years of hydrothermal activity at the Lost City vent field. *Science* 301:495–498.
13. Ludwig KA, Kelley DS, Butterfield DA, Nelson BK, Früh-Green GL (2006) Formation and evolution of carbonate chimneys at the Lost City Hydrothermal Field. *Geochim Cosmochim Acta* 70:3625–3645.
14. Fouquet Y, et al. (1993) Tectonic setting and mineralogical and geochemical zonation in the Snake Pit sulfide deposit (Mid-Atlantic Ridge at 23°N). *Econ Geol* 88:2018–2036.
15. Holm NG, Charlou JL (2001) Initial indications of abiogenic formation of hydrocarbons in the Rainbow ultramafic hydrothermal system, Mid-Atlantic Ridge. *Earth Planet Sci Lett* 191:1–8.
16. Sleep NH, Meibom A, Fridriksson T, Coleman RG, Bird DK (2004) H₂-rich fluids from serpentinization: Geochemical and biotic implications. *Proc Natl Acad Sci USA* 101:12818–12823.
17. Kelley DS, Früh-Green GL, Karson JA, Ludwig KA (2007) The Lost City hydrothermal field revisited. *Oceanography* 20:90–99.
18. DeChaine EG, Bates AE, Shank TM, Cavanaugh CM (2006) Off-axis symbiosis found: Characterization and biogeography of bacterial symbionts of *Bathymodiolus* mussels from Lost City hydrothermal vents. *Environ Microbiol* 8:1902–1912.
19. Shank TM, Buckman KL, Butterfield D, Kelley D (2006) Macrofaunal characterization of peridotite-hosted ecosystems associated with Lost City hydrothermal field. *Eos Trans AGU* 87(36):OS10–35 Abstract.
20. Gebruk AV, Galkin SV, Krylova EM, Vereshchaka AL, Vinogradov VM (2002) Hydrothermal fauna discovered at Lost City (30°N, Mid-Atlantic Ridge). *InterRidge News* 11:18–19.
21. Dara OM, Kuz'mina TG, Lein AY (2009) Mineral associations of the Lost Village and Lost City hydrothermal fields in the North Atlantic. *Oceanology* 49:688–696.
22. Le Bris N, Duperron S (2010) Chemosynthetic communities and biogeochemical energy pathways along the MAR: The case of *Bathymodiolus azoricus*. *Diversity of Hydrothermal Systems on Slow-Spreading Ocean Ridges*, eds PA Rona, CW Devey, J Dymont, and BJ Murton (American Geophysical Union, Washington, DC), Vol 188, pp 409–429.
23. Fiala-Medioni A, et al. (2002) Ultrastructural, biochemical, and immunological characterization of two populations of the mytilid mussels *Bathymodiolus azoricus* from the Mid-Atlantic Ridge: Evidence for a dual symbiosis. *Mar Biol* 141:1035–1043.
24. Duperron S, et al. (2006) A dual symbiosis shared by two mussel species, *Bathymodiolus azoricus* and *Bathymodiolus puteoserpentis* (Bivalvia: Mytilidae), from hydrothermal vents along the northern Mid-Atlantic Ridge. *Environ Microbiol* 8:1441–1447.
25. Riou V, et al. (2008) Influence of chemosynthetic substrates availability on symbiont densities, carbon assimilation and transfer in the dual symbiotic vent mussel *Bathymodiolus azoricus*. *Biogeosci Discuss* 5:2279–2304.
26. Desbruyères D, et al. (2001) Variations in deep-sea hydrothermal vent communities on the Mid-Atlantic Ridge near the Azores plateau. *Deep Sea Res Part 1* 48:1325–1346.
27. Konn C, et al. (2009) Hydrocarbons and oxidized organic compounds in hydrothermal fluids from Rainbow and Lost City ultramafic-hosted vents. *Chem Geol* 258:299–314.
28. Brazelton WJ, Schrenk MO, Kelley DS, Baross JA (2006) Methane- and sulfur-metabolizing microbial communities dominate the Lost City hydrothermal field ecosystem. *Appl Environ Microbiol* 72:6257–6270.
29. Brazelton WJ, et al. (2010) Archaea and bacteria with surprising microdiversity show shifts in dominance over 1,000-year time scales in hydrothermal chimneys. *Proc Natl Acad Sci USA* 107:1612–1617.
30. Cannat M, Fontaine F, Escartin J (2010) Serpentinization and associated hydrogen and methane fluxes at slow spreading ridges. *Diversity of Hydrothermal Systems on Slow Spreading Ocean Ridges*, eds PA Rona, CW Devey, J Dymont, and BJ Murton (American Geophysical Union, Washington, DC), Vol 188, pp 241–264.
31. Robinson LF, Belshaw NS, Henderson GM (2004) U and Th concentrations and isotope ratios in modern carbonates and waters from the Bahamas. *Geochim Cosmochim Acta* 68:1777–1789.
32. Ludwig KA, et al. (2011) U-Th systematics and ²³⁰Th ages of carbonate chimneys at the Lost City Hydrothermal Field. *Geochim Cosmochim Acta* 75:1869–1888.
33. Kuznetsov K, et al. (2006) ²³⁰Th/^U dating of massive sulfides from the Logatchev and Rainbow hydrothermal fields (Mid-Atlantic Ridge). *Geochronometria* 25:51–55.
34. Eickmann B, Bach W, Peckmann J (2009) Authigenesis of carbonate minerals in modern and Devonian ocean-floor hard rock. *J Geol* 117:307–323.
35. Ribeiro Da Costa I, Barriga FJAS, Taylor RN (2008) Late seafloor carbonate precipitation in serpentinites from the Rainbow and Saldanha sites (Mid-Atlantic Ridge). *Eur J Mineral* 20:173–181.
36. Buchardt B, et al. (1997) Submarine columns of ikaite tufa. *Nature* 390:129–130.
37. Selleck BW, Carr PF, Jones BG (2007) A review and synthesis of glendonites (pseudomorphs after ikaite) with new data: assessing applicability as recorders of ancient coldwater conditions. *J Sediment Res* 77:980–991.
38. Mével C (2003) Serpentinization of abyssal peridotites at mid-ocean ridges. *CR Geosci* 335:825–852.
39. Haggerty JA (1991) Evidence from fluid seeps atop serpentine seamounts in the Mariana forearc: Clues for emplacement of the seamounts and their relationship to forearc tectonics. *Mar Geol* 102:293–309.
40. Kato K, Wada H, Fujioka K (1998) Carbon and oxygen isotope composition of carbonate chimney from Mariana forearc seamount. *JAMSTEC Deep Sea Res* 14:213–222.
41. Yamanaka T, et al. (2003) Stable isotope evidence for a putative endosymbiont-based lithotrophic *Bathymodiolus* sp. mussel community atop a serpentine seamount. *Geomicrobiol J* 20:185–197.
42. Abrajano TA, et al. (1990) Geochemistry of reduced gas related to serpentinization of the Zambas ophiolite, Philippines. *Appl Geochem* 5:625–630.
43. Lilley MD, et al. (1993) Anomalous CH₄ and NH₄⁺ concentrations at unsedimented mid-ocean-ridge hydrothermal system. *Nature* 364:45–47.
44. Charlou JL, et al. (2010) High production and fluxes of H₂ and CH₄ and evidence of abiogenic hydrocarbon synthesis by serpentinization in ultramafic-hosted hydrothermal systems on the Mid-Atlantic Ridge. *Diversity of Hydrothermal Systems on Slow-Spreading Ocean Ridges*, eds PA Rona, CW Devey, J Dymont, and BJ Murton (American Geophysical Union, Washington, DC), pp 265–296.
45. Proskurowski G, et al. (2008) Abiogenic hydrocarbon production at Lost City hydrothermal field. *Science* 319:604–607.
46. Webley PA, Tester JW (1991) Fundamental kinetics of methane oxidation in supercritical water. *Energy Fuels* 5:411–419.
47. Valentine DL, Reeburgh WS (2000) New perspectives on anaerobic methane oxidation. *Environ Microbiol* 2:477–484.
48. Proskurowski G, Lilley MD, Olson EJ (2008) Stable isotopic evidence in support of active microbial methane cycling in low-temperature diffuse flows vents at 9°50'N East Pacific Rise. *Geochim Cosmochim Acta* 72:2005–2023.
49. Whiticar MJ, Faber E (1986) Methane oxidation in sediment and water column environments— isotopic evidence. *Org Geochem* 10:759–768.
50. Templeton AS, Chu KH, Alvarez-Cohen L, Conrad ME (2006) Variable carbon isotope fractionation expressed by aerobic CH₄-oxidizing bacteria. *Geochim Cosmochim Acta* 70:1739–1752.
51. Comtet T, Desbruyères D (1998) Population structure and recruitment in mytilid bivalves from the Lucky Strike and Menez Gwen hydrothermal vent fields (37°17'N and 37°50'N on the Mid-Atlantic Ridge). *Mar Ecol Prog Ser* 163:165–177.
52. Southward EC, Gebruk AV, Kennedy H, Southward AJ, Chevaldonné P (2001) Different energy sources for three symbiont-dependent bivalve mollusks at the Logatchev hydrothermal site (Mid-Atlantic Ridge). *J Mar Biol Assoc UK* 81:655–661.
53. Warén A, Bouchet P (2001) Gastropoda and monoplacophora from hydrothermal vents and seeps; new taxa and records. *Veliger* 44:116–231.
54. Taylor JD, Williams ST, Glover EA (2007) Evolutionary relationships of the bivalve family Thyasiridae (Mollusca: Bivalvia), monophyly and superfamily status. *J Mar Biol Assoc UK* 87:565–574.
55. Lartaud F, et al. (2010) Fossil clams from a serpentinite-hosted sedimented vent field near the active smoker complex Rainbow (MAR, 26°13'N): insight into the biogeography of vent fauna. *Geochim Geophys Geosyst* 11:Q0AE01.
56. Gebruk AV, Chevaldonné P, Shank T, Lutz RA, Vrijenhoek RC (2000) Deep-sea hydrothermal vent communities of the Logatchev area (14°45'N, Mid-Atlantic Ridge): Diverse biotopes and high biomass. *J Mar Biol Assoc UK* 80:383–393.
57. Oliver PG, Holmes AM (2006) New species of Thyasiridae (Bivalvia) from chemosynthetic communities in the Atlantic Ocean. *J Conchol* 39:175.
58. Charlou JL, Donval JP, Fouquet Y, Jean-Baptiste P, Holm N (2002) Geochemistry of high H₂ and CH₄ vent fluids issuing from ultramafic rocks at the Rainbow hydrothermal field (36°14'N, MAR). *Chem Geol* 191:345–359.
59. Childress JJ, Fisher CR, Favuzzi JA, Sanders NK (1991) Sulfide and carbon-dioxide uptake by the hydrothermal vent clam, *Calyptogena magnifica*, and its chemoautotrophic symbionts. *Physiol Zool* 64:1444–1470.
60. Früh-Green GL, Connolly JA, Plas A (2004) Serpentinization of oceanic peridotites: Implications for geochemical cycles and biological activity. *The Subsurface Biosphere at Mid-Ocean Ridges*, eds WSD Wilcock, EF DeLong, DS Kelley, JA Baross, and SC Cary (American Geophysical Union, Washington, DC), Vol 144.
61. Ildefonse B, et al. (2007) Oceanic core complexes and crustal accretion at slow-spreading ridges. *Geology* 35:623–626.
62. Hopkinson L, Beard JS, Boulter CA (2004) The hydrothermal plumbing of a serpentinite-hosted detachment: Evidence from the West Iberia non-volcanic rifted continental margin. *Mar Geol* 204:301–315.
63. Alt JC, Shanks WC (2006) Stable isotope compositions of serpentinite seamounts in the Mariana forearc: serpentinization processes, fluid sources and sulfur metasomatism. *Earth Planet Sci Lett* 242:272–285.
64. Sponheimer M, Lee-Thorp JM (1999) Isotopic evidence for the diet of an early Hominid, *Australopithecus africanus*. *Science* 283:368–370.
65. Ségalen L, Lee-Thorp JM (2009) Palaeoecology of late Early Miocene fauna in the Namib based on ¹³C/¹²C and ¹⁸O/¹⁶O ratios of tooth enamel and ratite eggshell carbonate. *Palaeogeogr Palaeoclimatol Palaeoecol* 277:191–198.
66. Robinson LF, Henderson GM, Slowey NC (2002) U-Th dating of marine isotope stage 7 in Bahamas slope sediments. *Earth Planet Sci Lett* 196:175–187.
67. Edwards RL, Chen JH, Wasserburg GR (1986) ²³⁸U-²³⁴U-²³⁰Th-²³²Th systematics and the precise measurement of time over the past 500,000 years. *Earth Planet Sci Lett* 81:175–192.
68. Bayon G, Henderson GM, Bohn M (2009) U-Th stratigraphy of a cold seep carbonate crust. *Chem Geol* 260:47–56.